Blueprint for antimicrobial hit discovery targeting metabolic networks

Y. Shen[a,b,1], J. Liu[b,1], G. Estiu[a], B. Isin[b], Y-Y. Ahn[c,d], D-S. Lee[c,d,4], A-L. Barabási[c,d], V. Kapatral[e], O. Wiest[a,2,3], and Z. N. Oltvai[b,2,3]

[a]Department of Chemistry and Biochemistry, University of Notre Dame, Notre Dame, IN, 46556; [b]Departments of Pathology and Computational Biology, University of Pittsburgh, Pittsburgh, PA, 15261; [c]Center for Complex Network Research and Departments of Physics, Biology, and Computer Science, Northeastern University, Boston, MA 02115; [d]Center for Cancer Systems Biology, Dana-Farber Cancer Institute, Boston, MA 02115; and [e]Integrated Genomics, Inc., Chicago, IL 60612

Advances in genome analysis, network biology, and computational chemistry have the potential to revolutionize drug discovery by combining system-level identification of drug targets with the atomistic modeling of small molecules capable of modulating their activity. To demonstrate the effectiveness of such a discovery pipeline, we deduced common antibiotic targets in *Escherichia coli* and *Staphylococcus aureus* by identifying shared tissue-specific or uniformly essential metabolic reactions in their metabolic networks. We then predicted through virtual screening dozens of potential inhibitors for several enzymes of these reactions and showed experimentally that a subset of these inhibited both enzyme activities in vitro and bacterial cell viability. This blueprint is applicable for any sequenced organism with high-quality metabolic reconstruction and suggests a general strategy for strain-specific antiinfective therapy.

antibiotics | flux balance analysis | virtual screening

The deciphering of genomes from a variety of organisms holds the promise of significantly increasing the speed and efficiency of drug discovery. The challenge to find "druggable" targets (1) that will have an effect in the complex interaction network of a living organism has been only partially met by genomics and functional genomics approaches (2). For example, systematic gene deletion studies have been widely used to identify essential genes whose protein product could serve as potential antibiotic targets in a given bacterium. This approach yields only growth-condition-specific results, as a molecular target that is found to be essential in one specific environment may not be essential in others. To overcome these limitations and to couple target identification to the identification of small molecules that can affect them, cellular network analysis and computational chemistry approaches may prove highly efficient and scalable methods. By using entirely computational methods in the initial steps of drug discovery, the more expensive and time-consuming experimental methods could be applied in a more focused fashion to smaller sets of targets and hits. Although the potential time and resource savings of this strategy are widely acknowledged and have already yielded interesting results in individual aspects of drug discovery (3, 4), so far there have been no successful examples where computational methods were integrated seamlessly to develop hits toward targets identified and validated by using genomic and systems-level methods.

Antibiotic drug resistance significantly eroded the effectiveness of currently available antimicrobial drugs toward disease-causing bacteria (5). As a consequence, today the yearly mortality rate in the United States due to multidrug-resistant *Staphylococcus aureus* infections is higher than that due to AIDS (6). Here, we provide a proof-of-principle demonstration that the combined use of bacterial metabolic network analysis with virtual screening and subsequent experimental verification is an effective method for the simultaneous identification of novel antimicrobial targets and inhibitory small molecules against them. Fig. 1 displays the main steps of our protocol. This blueprint for the rapid discovery of new antibiotic hits against new and specific molecular targets addresses a critical need and, with adjustment, is applicable to all diseases involving alterations in various biochemical reaction networks.

Results

Identification of Antimicrobial Targets by the Analysis of Bacterial Metabolic Networks. We performed flux balance analysis (FBA) to identify the essential metabolic reactions of *Escherichia coli* MG1655 by using a recent metabolic network reconstruction of this Gram-negative model organism (7). This analysis predicted 38 metabolic reactions as having nonzero flux under all growth conditions and being indispensable for the synthesis of the full set of biomass components in this bacterium. In the absence of isozymes or compensatory (nonspecific) enzymatic activities, the enzymes catalyzing these reactions are expected to be essential under all conditions and thus represent potential targets for antimicrobial drug discovery (8, 9). A high fraction of the enzymes catalyzing the 38 predicted indispensable reactions were found to be essential in three previous genome-scale gene deletion studies (10–12) (Table S1). Seven of these indispensable reactions are shared among *E. coli* MG1655 and 13 *S. aureus* strains (9), with the enzymes of five of them being experimentally validated as essential in at least one of the *E. coli* gene deletion studies (Table 1). These reactions are not distributed randomly within the metabolism but cluster into distinct metabolic pathways that are known to play key roles in bacterial cell wall, amino acid, and porphyrin biosyntheses.

Some reactions are indispensable only in one type of bacterium. For example, most enzymes of the type-II bacterial fatty-acid biosynthesis (FAS II) pathways (13) are predicted as unconditionally essential in 13 *S. aureus* species (9) but not in *E. coli* MG1655, which has several transporters that enable it to take up fatty acids directly from the environment (7). Yet, in standard (fatty-acid-free) growth media, the inactivation of most FAS II enzymes renders *E. coli* cells inviable (Fig. 2A), and the loss of cell viability can be countered by the addition of unsaturated fatty acids to the growth media (14, 15). In a recent intraperitoneal infection model with Gram-positive *Streptococcus agalactiae*, inactivation of FAS II enzymes also proved ineffective (16), suggesting that pharmaceutical inhibition of FAS II enzymes may not be a feasible strategy for the treatment of systemic bacterial infections. How-

BIOPHYSICS AND COMPUTATIONAL BIOLOGY

Fig. 1. Blueprint for antimicrobial hit identification. Genome-scale metabolic network reconstruction and subsequent FBA identify those reactions that are required for biomass formation under all growth conditions (*Left*). The enzymes catalyzing the essential reactions are docked against a small-molecule library to identify their potential small-molecule inhibitors (*Center*). The potential inhibitors are then tested experimentally (*Right*).

ever, these enzymes may be suitable targets for the eradication of cutaneous antibiotic-resistant bacterial colonizations or for treating cutaneous infections caused by, e.g., methicillin-resistant *S. aureus* (17, 18).

Virtual Screening of Small-Molecule Compounds Against Enzymes of Bacterial Fatty-Acid Biosynthesis. We considered enzymes of the FAS II pathway with a uniformly lethal deletion phenotype in *E. coli* as potential high-confidence targets, whereas those with at least one mismatch in the *E. coli* deletion phenotype data, or having isozymes, were considered lower-confidence targets (Fig. 2*A*). We first focused on the malonyl-CoA-acyl carrier protein transacylase (MCAT, FabD), which catalyzes the first committed step in the initiation step of the fatty-acid biosynthesis pathway (Fig. 2*A*) and which shows high sequence conservation

Table 1. Enzymes catalyzing essential metabolic reactions conserved between *E. coli* and *S. aureus* strains may represent novel antibiotic targets

	Gerdes	Baba	Kang
aminosugars metabolism			
murB		■	
amino acid biosynthesis			
aroA			
aroC			
porphyrin metabolism			
hemB	■		■
hemD	■	■	■
methionine metabolism			
metK	■	■	■
mtn	■		■
fatty acid biosynthesis			
fabD	■	■	■
fabH	■	■	■
fabF		■	
fabG	■	■	■
accA	■	■	■
accD		■	■

among the sixteen most common human bacterial pathogens (Fig. S1). Crystal structures of bacterial FabDs (19–22) and their mammalian orthologs are available (23). We identified 15 potential inhibitors of FabD (FDi1–15) through virtual screening. Briefly, the ZINC lead library (24) containing $\sim 10^6$ small molecules prefiltered for drug-like properties was docked either to the crystal structures of *E. coli* FabD or to a FabD homology model derived for *S. aureus* N315 by using successively more accurate scoring functions followed by manual inspection of poses and rescoring by MM-PBSA (molecular mechanics Poisson–Boltzmann/surface area) calculations from an ensemble of molecular dynamics (MD) simulations (see Supporting Information for details) (25). Fig. 2*B* shows two representative potential inhibitors, FDi2 and FDi14, bound to the active site of *E. coli* FabD. They exemplify the pharmacophore that is further confirmed by other docked structures and the putative binding mode of the natural substrate (21). The close-up of FDi2 in the active site of *E. coli* FabD illustrates the relevant interactions (Fig. 2*C*). The carboxylate acts as a phosphate isostere and interacts with the catalytic Arg[117], Leu[93], and Gln[11], respectively. A polar linker to a thiophene ring enables stacking against His[91] and occupation of a hydrophobic pocket by a benzene moiety. Similar interactions are found for FDi10 in the active site of *S. aureus* FabD (Fig. 2*D*). Further information on other compounds can be found in Tables S3 and S5.

E. coli FabD shares ~34% similarity with its human mitochondrial ortholog (Protein Data Bank ID 2c2n) with their backbones being almost superimposable (Fig. S1), but human mitochondrial FabD (shown in blue in Fig. 2*B*) has a much smaller active site than *E. coli* FabD (shown in red in Fig. 2*B*). Thus, FDi14 could potentially bind to the active site of human mitochondrial FabD, but FDi2 is predicted to be unable to do so. Thus, the active sites of human mitochondrial and *E. coli* FabD are sufficiently different for small molecules to selectively inhibit bacterial FabDs.

A particular strength of the approach used here is that it has an inherently systems-wide view rather than targeting a single enzyme, as is done in traditional drug design. If an enzyme is essential by itself (e.g., FabD), its specific inhibitors should be able
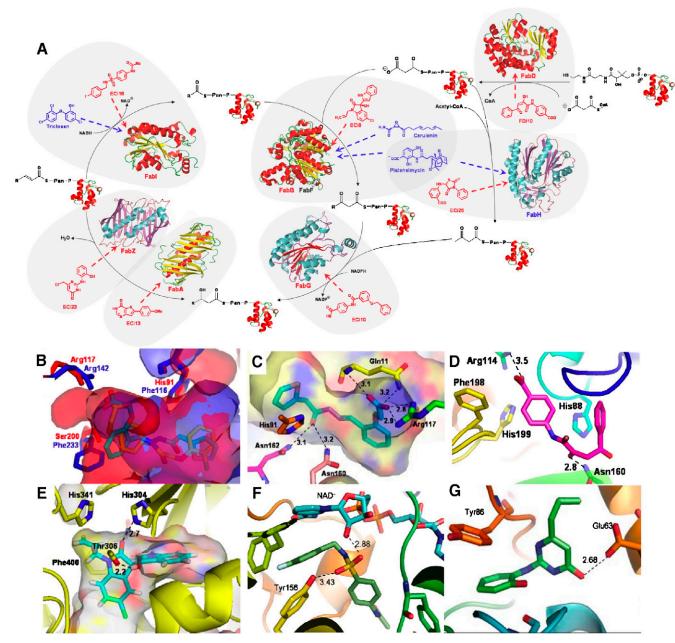
Fig. 2. Small-molecule inhibitors of FAS II enzymes. (*A*) FAS II pathway and structures of select, existing antimicrobials (blue) and some of the newly identified small-molecule inhibitors (red) against their target enzymes. The structures used for the virtual screenings are also shown. *E. coli* viability data for FAS II pathway enzymes from three independent gene deletion studies are indicated: uniformly essential (red), dispensable (black), or conflicting deletion phenotype (blue) enzymes. (*B*) The active site of *E. coli* FabD (Protein Data Bank: 2g2z, in red) superimposed on human mitochondrial MCAT (Protein Data Bank: 2c2n, in blue) with two docked ligands: FDi2 (cyan) and FDi14 (yellow). (*C–G*) Interactions of selected inhibitors in the active sites of their respective targets: (*C*) FDi2 in *E. coli* FabD after 8 ns MD; (*D*) FDi10 docked to *S. aureus* FabD homology model built from *E. coli* FabD; (*E*) ECi8 docked to *S. aureus* FabF; (*F*) ECi16 docked to *E. coli* FabI; and (*G*) ECi23 in a homology model of *E. coli* FabZ after 8 ns MD.

to kill bacteria. Similarly, isozyme pairs, such as FabB and FabF in *E. coli*, are also promising targets if both of them are targeted simultaneously. For example, FAS II inhibitors thiolactomycin, cerulenin, or platensimycin are known to simultaneously inhibit both FabB and FabF (Fig. 2*A*) and have broad-spectrum antibacterial activity (26).

We therefore screened all remaining enzymes of the FAS II pathway (FabH, FabB/F, FabG, FabA/Z, and FabI) (Fig. 2*A*) by using ligand-bound crystal structures or homology models (Table S2). This computational procedure yielded 26 small molecules that can potentially inhibit the FAS II elongation cycle enzymes (ECi1–26). Because several of the enzymes are function-

ally redundant in some organisms and the product of one step is the substrate of the next, the binding sites share many similarities. As a result, similar common binding moieties, such as a phosphate isostere, a hydrogen binding polar group, and a nonpolar ring system in a similar position emerge from the screens, which suggests the possibility of inhibiting several targets simultaneously. This concept of polypharmacology has been successfully applied in a number of cases before (27) and is part of the inherent design in our case.

Representative results from these studies are shown in Fig. 2*E*–*G*, whereas the remaining structures are summarized in Figs. S3 and S4, and Table S3 in the Supporting Information.

ECi8 is predicted to inhibit both FabB and FabF (Fig. 2E), shares the binding characteristics of known inhibitors (26, 28), and has a good shape complementarity to the active sites of both enzymes. In agreement with the hypothesis outlined above, cross-docking shows that ECi8 also has good poses and scores for binding to FabI and FabG, the adjacent enzymes in the elongation cycle.

The NADPH- and NADH-dependent reductases FabG and FabI have similar active sites, and several inhibitors exist for the latter, including triclosan (Fig. 2A). The most promising inhibitor identified by virtual screening, ECi16, shows similar interactions as triclosan: The fluorophenyl ring π-stacks with the oxidized nicotinamide, whereas the oxygen atoms of the sulfamide group participate in hydrogen bond interactions with the conserved active site tyrosine (Y^{156} in E. coli FabI) and the 2′ hydroxyl of NAD^+ (Fig. 2F).

The active sites of the dehydratases FabA and FabZ are formed along the dimer interface, with the critical His^{70} and Asp^{84}(FabA)/Glu^{63}(FabZ) contributed by different monomers. The virtual screening identifies the interaction with Asp^{84}/Glu^{63} as the most relevant for inhibitor binding. Fig. 2G depicts this interaction in the binding of ECi23 in the FabZ active site, where the inhibitor is also stabilized by π-stacking with Tyr^{86}. A complete list of the identified potential FabD and elongation cycle inhibitors is presented in Table S3.

Testing the Effect of Predicted Inhibitors by Enzyme Assays and Cell-Based Experiments. To experimentally validate the inhibitory effect of the 41 compounds selected from the 10^6 library members on bacterial fatty-acid enzymes, we set up two separate published enzyme screening assays: one for testing FabD activity (29) and the other for testing the inhibition of the elongation cycle (30). For the FabD screening assay, we cloned the E. coli FabD and its protein substrate, AcpP, into a prokaryotic expression vector, induced their expression, and purified them to homogeneity. We then tested the purified FabD's activity in the absence or presence of the predicted inhibitors (see Table S4 and the Supporting Information for details). Of the 15 predicted inhibitors, we found that five of them (FDi2, 7, 8, 10, and 11) strongly and three of them (FDi12, 14, and 15) weakly inhibited FabD activity (for details, see the Supporting Information).

We also tested the effect of the 26 small molecules that are predicted to block the activity of various elongation cycle enzymes by using an established, fractionated cytoplasmic protein extract-based elongation cycle assay (30) with slight modifications (see Supporting Information). ECi8, 21, 23, and 26 have shown strong and ECi10, 11, 12, 13, 14, and 16 weak inhibitions toward the FAS II elongation cycle enzymes (Fig. S5). Although the nature of the assay does not allow the precise differentiation of all FAS II targets, the results are consistent with the targets being inhibited by their computationally predicted inhibitors in a dose-dependent fashion (Fig. S5d). Of the 41 potential inhibitors identified in the virtual screening protocol, eight were highly and nine were weakly active. For each enzyme of the FAS II elongation cycle, we could identify at least one validated inhibitor (see Tables S3 and S5 for details). This exceptionally high hit rate of >40% is remarkable considering the simple physical models used in the scoring functions and is significantly higher than what is typically obtained in virtual screening. Consequently, MM-PBSA rescoring is, at least for the present systems, able to describe side chain flexibility and hydrophobic effects and thus represents a significant improvement for virtual screening (25). It is expected that explicit treatment of entropy could further improve the hit rate, albeit at a significant computational cost.

Next, we examined the effect of these compounds on bacterial cell viability by performing disc inhibition assays against two E. coli strains (MG1655 and a random patient isolate) and three S. aureus strains (S. aureus Mu50, USA300, and a strain isolated from a patient) by using standard procedures (31). Because it was reported that serum is a rich source of unsaturated fatty acids excluding the use of FAS II inhibitors for the treatment of systemic infections (16), we performed the experiments both on LB-agar and LB-agar plus 10% human serum plates (Fig. 3).

When using standard LB-agar plates (Fig. 3A and blue-shaded columns in Table 2) among the identified FabD and elongation cycle, enzyme inhibitors FDi8, 11, 12, and 15 did not show any inhibitory effect in this whole cell assay. In contrast, FDi2, 7, 10, and 14 and ECi8 and 23 were found to be active against all five strains tested, although their zone of inhibition was different both quantitatively and qualitatively for different strains (Fig. 3). ECi16 displayed only a minor inhibitory effect on the E. coli patient and MG1655 strains, while the remaining inhibitors, including ECi11, were without effect (Fig. 3). Of note, even though S. aureus Mu50 and USA300 strains are methicillin- and vancomycin-resistant opportunistic pathogens, respectively, in the Mu50 strain FDi10 and ECi8 and 23 displayed a clear zone of inhibition that was even stronger than the one caused by ampicillin (blue-shaded column in Table 2). In the presence of unsaturated fatty acids (Fig. 3B and pink-shaded columns in Table 2), FDi2 and ECi16 completely lost their inhibitory function, while FDi7 and 14 and ECi23 displayed partial inhibitory activities. In contrast, FDi10 and ECi8 retained most of their activity. These findings are consistent with the notion that the presence of unsaturated fatty acids can indeed bypass the need for FAS II enzymes (16) and suggest that some of the identified inhibitors may also possess off-target growth inhibitory effects.

To further test if the identified inhibitors react with their targets' human orthologs and/or cause toxicity in human cells through off-target effects, we employed 3-(4,5-dimethylthiazol-2-yl)-2,5-diphenyl tetrazolium bromide (MTT) cell viability and trypan blue exclusion assays to examine the effect of potential inhibitors on mammalian cells. Normal human BJ foreskin fibroblast cells immortalized by the catalytic subunit of human telomerase (32) were utilized for this purpose. After treating the cells with 400 μg/mL of each inhibitor, we found that FDi2 displayed comparable MTT activity and live cell numbers with the DMSO solvent control, indicating that it has no toxicity or inhibitory effect on cell viability (Table 2). In contrast, similar to the effect of cerulenin and triclosan, ECi8 and 23 completely blocked MTT activity and killed the fibroblast cells. The other inhibitors, including FDi10, FDi14, and ECi16, showed partial inhibition on mammalian cells and could potentially be further optimized for antibacterial selectivity. Of note, these experimental results are in agreement with the docking predictions for the bacterial selectivity (or lack of) of FabD inhibitors FDi2 and FDi14 (Fig. 2B).
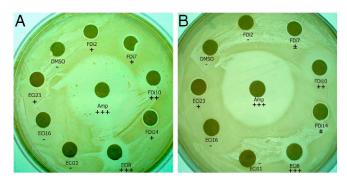

Fig. 3. The inhibitory effects of small molecules against an S. aureus patient strain. Representative disc inhibition assay results (except ECi11) on (A) an LB-agar plate and (B) an LB-agar plate plus 10% human serum together with positive [Ampicillin (Amp)] and negative solvent (DMSO) controls are shown.

Table 2. Summary of bacterial disc inhibition and human fibroblast toxicity assay results

	FabD (FD)								Elongation Cycle (EC)								Controls			
	i2		i7		i10		i14		i8		i11		i16		i23		Amp		DMSO	
S. aureus Mu50	+	-	+	-	++	+	+	-	++	+	-	-	-	-	-	-	±	+	-	-
S. aureus patient	+	-	+	±	++	++	+	±	+++	+++	-	-	-	-	+	+	+++	+++	-	-
S. aureus USA300	+	-	++	-	++	++	+	±	+++	+++	-	-	-	-	+	-	+++	+++	-	-
E. coli MG1655	+	-	+	-	+	-	+	±	+	+	-	-	+	ND	+	+	+++	+++	-	-
E. coli patient	+	-	+	-	+	-	+	±	+	±	-	-	+	-	+	-	+++	+++	-	-
Mammalian cell toxicity																	Triclosan		Cerulenin	
MTT activity	-		±		±		±		+++		±		±		+++		±		+++	
Trypan blue excl.	-		+		+		+		+++		+		+		+++		+++		+++	

LL+: Weak inhibition; ++: weak inhibition plus zone of partial inhibition;
+ + +: strong inhibition; ±: partial inhibition; –: no inhibition. The blue shad-

Discussion

The promise of genome projects, functional genomics studies, and network biology in providing new molecular targets for pharmaceutical intervention in different disease states is now becoming a reality (33, 34). This pharmaceutical intervention is particularly important in the area of infectious diseases, where the dual problems of multidrug resistance and the scarcity of effective therapy for a large number of diseases are well recognized. Although genome-scale gene deletions have been used for antimicrobial drug target identification, this experimental strategy is time-consuming and provides only growth-condition-specific results. In some organisms that are hard to cultivate, such as *Plasmodium falciparum* or *Mycobacterium tuberculosis*, it is technically not feasible. With the large number of sequenced genomes of disease-causing prokaryotes (bacteria) and eukaryotes (fungi, malaria, trypanosomes, etc.), the approach introduced here, which can effectively start from the sequence, represents an increasingly attractive alternative.

From a more general perspective, a key aim of network medicine is to reconstitute the physiological network states of cells in a systematic and computable fashion (35). In the case of microbial infections, however, this aim entails the drug therapy-induced alteration of network states that are deleterious to the infectious organism, including its ability to synthesize biomass constituents or virulence factors, or to the function of its key cellular constituents (e.g., the ribosome) (Fig. 4A). The blueprint we demonstrate here combines genomic information and network biology-based strain-specific molecular target identification (Fig. 4B, *Left*) with computational ranking of ∼10^6 small molecules to identify potential antimicrobial scaffolds against the identified target enzymes (Fig. 4B, *Right*). In turn, these define the chemical subspace for organism- or strain-specific lead development using traditional or structure-based methods of medicinal chemistry. This strategy could easily be extended to other pathways found to be essential for bacteria, such as those regulating the generation of reactive oxygen intermediates that can potentiate the activity of individual antibiotic compounds (36–38).

In routine molecular diagnostics full genome analysis using massively parallel sequencing technologies coupled to network medicine is likely to be first employed for microorganisms, which have relatively small genomes, where genome analysis, metabolic
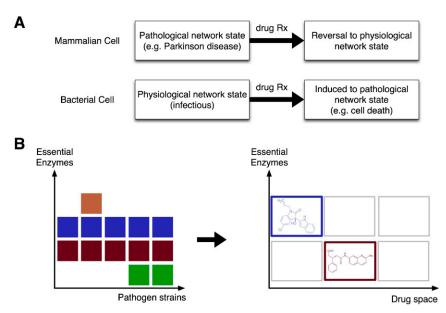

Fig. 4. Approach to personalized antiinfective therapy. (*A*) For most diseases the aim of network medicine is to reestablish a physiological network state in a personalized fashion by affecting a ranked list of molecular targets, but for antimicrobial therapy the aim is just the opposite. (*B*) For each pathogenic bacterial strain, the list of essential enzymes in a given strain can be calculated (*Left*). For each target enzyme, an experimentally validated small-molecule hit that inhibits a given strain/essential enzyme combination defines the chemical subspace for subsequent compound optimization (*Right*).

reconstruction, and subsequent network analysis are now routine (39) and where the benefits of isolate-specific treatments have long been well-established. Therefore, the comparison of a fully sequenced *S. aureus* patient isolate to a compendium of a full genome sequence plus high quality metabolic reconstruction of, e.g., 1,000 *S. aureus* strains will allow the deployment of strain-optimized antimicrobial therapy, providing that a corresponding, well characterized pharmaceutical library [including information on off-target effects (40)] has also been established. With rapidly increasing computational power, computer-aided drug discovery, disease diagnosis, and tailored therapy are now becoming increasingly plausible.

Materials and Methods

Identification of Essential Metabolic Reactions in *E. coli*. FBA to identify the essential metabolic reactions of *E. coli* MG1655 by using its recent metabolic network reconstruction (7) was performed as previously described (9) and as detailed in the Supplementary Information.

Computational Chemistry Protocols for Hit Identification. Virtual screening using the ZINC lead library (24) and subsequent manual inspection of poses and rescoring by MM-PBSA calculations from an ensemble of MD simulations were performed, as previously described (25), and are detailed in the Supplementary Information.

Enzyme Inhibition Assays, Bacterial Growth, and Cytotoxicity Studies. Two *E. coli* (MG1655 and patient isolate) and three *S. aureus* (Mu50, USA300, and patient isolate) strains and human fibroblast cells were used. The experimental details of the in vitro enzyme assays, bacterial growth inhibition, and mammalian cell toxicity tests are detailed in the Supplementary Information.

1. Russ AP, Lampel S (2005) The druggable genome: An update. *Drug Discovery Today*, 10:1577–1579.
2. Orth AP, Batalov S, Perrone M, Chanda SK (2004) The promise of genomics to identify novel therapeutic targets. *Expert Opin Ther Targets*, 8:587–596.
3. Gardner TS, di Bernardo D, Lorenz D, Collins JJ (2003) Inferring genetic networks and identifying compound mode of action via expression profiling. *Science*, 301:102–105.
4. Lamb J, et al. (2006) The connectivity map: Using gene-expression signatures to connect small molecules, genes, and disease. *Science*, 313:1929–1935.
5. Fischbach MA, Walsh CT (2009) Antibiotics for emerging pathogens. *Science*, 325:1089–1093.
6. Klevens RM, et al. (2007) Invasive methicillin-resistant *Staphylococcus aureus* infections in the United States. *JAMA, J Am Med Assoc*, 298:1763–1771.
7. Feist AM, et al. (2007) A genome-scale metabolic reconstruction for *Escherichia coli* K-12 MG1655 that accounts for 1260 ORFs and thermodynamic information. *Mol Syst Biol*, 3:121.
8. Almaas E, Oltvai ZN, Barabási A-L (2005) The activity reaction core and plasticity of metabolic networks. *PLoS Comput Biol*, 1(e68):61–67.
9. Lee D-S, et al. (2009) Comparative genome-scale metabolic reconstruction and flux balance analysis of multiple *Staphylococcus aureus* genomes identify novel antimicrobial drug targets. *J Bacteriol*, 191:4015–4024.
10. Baba T, et al. (2006) Construction of *Escherichia coli* K-12 in-frame, single-gene knockout mutants: The Keio collection. *Mol Syst Biol*, 2 2006.0008.
11. Gerdes SY, et al. (2003) Experimental determination and system-level analysis of essential genes in *Escherichia coli* MG1655. *J Bacteriol*, 185:5673–5684.
12. Kang Y, et al. (2004) Systematic mutagenesis of the *Escherichia coli* genome. *J Bacteriol*, 186:4921–4930.
13. Zhang Y-M, Rock CO (2008) Membrane lipid homeostasis in bacteria. *Nat Rev Microbiol*, 6:222–233.
14. Campbell JW, Cronan JE (2001) *Escherichia coli* FadR positively regulates transcription of the fabB fatty acid biosynthetic gene. *J Bacteriol*, 183:5982–5990.
15. Harder ME, Ladenson RC, Schimmel SD, Silbert DF (1974) Mutants of *Escherichia coli* with temperature-sensitive malonyl coenzyme A-acyl carrier protein transacylase. *J Biol Chem*, 249:7468–7475.
16. Brinster S, et al. (2009) Type II fatty acid synthesis is not a suitable antibiotic target for Gram-positive pathogens. *Nature*, 458:83–86.
17. Jones PG, Sura T, Harris M, Strother A (2003) Mupirocin resistance in clinical isolates of *Staphylococcus aureus*. *Infect Control Hosp Epidemiol*, 24:300–301.
18. Kazakova SV, et al. (2005) A clone of methicillin-resistant *Staphylococcus aureus* among professional football players. *N Engl J Med*, 352:468–475.
19. Keatinge-Clay AT, et al. (2003) Catalysis, specificity, and ACP docking site of *Streptomyces coelicolor* malonyl-CoA:ACP transacylase. *Structure*, 11:147–154.
20. Li Z, et al. (2007) The crystal structure of MCAT from Mycobacterium tuberculosis reveals three new catalytic models. *J Mol Biol*, 371:1075–1083.
21. Oefner C, Schulz H, D'Arcy A, Dale GE (2006) Mapping the active site of *Escherichia coli* malonyl-CoA-acyl carrier protein transacylase (FabD) by protein crystallography. *Acta Crystallogr, Sect D: Biol Crystallogr*, 62:613–618.
22. Serre L, Verbree EC, Dauter Z, Stuitje AR, Derewenda ZS (1995) The *Escherichia coli* malonyl-CoA:acyl carrier protein transacylase at 1.5-A resolution. Crystal structure of a fatty acid synthase component. *J Biol Chem*, 270:12961–12964.
23. Maier T, Leibundgut M, Ban N (2008) The crystal structure of a mammalian fatty acid synthase. *Science*, 321:1315–1322.
24. Irwin JJ, Shoichet BK (2005) ZINC—A free database of commercially available compounds for virtual screening. *J Chem Inf Model*, 45:177–182.
25. Thompson DC, Humblet C, Joseph-McCarthy D (2008) Investigation of MM-PBSA rescoring of docking poses. *J Chem Inf Model*, 48:1081–1091.
26. Wang J, et al. (2006) Platensimycin is a selective FabF inhibitor with potent antibiotic properties. *Nature*, 441:358–361.
27. Lehár J, Stockwell BR, Giaever G, Nislow C (2008) Combination chemical genetics. *Nat Chem Biol*, 4:674–681.
28. Wang J, et al. (2007) Discovery of platencin, a dual FabF and FabH inhibitor with in vivo antibiotic properties. *Proc Natl Acad Sci USA*, 104:7612–7616.
29. Molnos J, Gardiner R, Dale GE, Lange R (2003) A continuous coupled enzyme assay for bacterial malonyl-CoA:acyl carrier protein transacylase (FabD). *Anal Biochem*, 319:171–176.
30. Kodali S, Galgoci A, Singh SB, Wang J (2006) Gel-elongation assay for type II fatty acid synthesis. *Nat Protoc* 10.1038/nprot.2006.1134.
31. Woods GL, Washington JA (1995) Antibacterial susceptibility tests: Dilution and disk diffusion methods. *Manual of Clinical Microbiology*, ed Murray PR (ASM Press, Washington, DC).
32. Hahn WC, et al. (1999) Creation of human tumour cells with defined genetic elements. *Nature*, 400:464–468.
33. Schadt EE, et al. (2005) An integrative genomics approach to infer causal associations between gene expression and disease. *Nat Genet*, 37:710–717.
34. Yang X, et al. (2009) Validation of candidate causal genes for obesity that affect shared metabolic pathways and networks. *Nat Genet*, 41:415–423.
35. Pawson T, Linding R (2008) Network medicine. *FEBS Lett*, 582:1266–1270.
36. Dwyer DJ, Kohanski MA, Collins JJ (2009) Role of reactive oxygen species in antibiotic action and resistance. *Curr Opin Microbiol*, 12:482–489.
37. Kohanski MA, Dwyer DJ, Hayete B, Lawrence CA, Collins JJ (2007) A common mechanism of cellular death induced by bactericidal antibiotics. *Cell*, 130:797–810.
38. Kohanski MA, Dwyer DJ, Wierzbowski J, Cottarel G, Collins JJ (2008) Mistranslation of membrane proteins and two-component system activation trigger antibiotic-mediated cell death. *Cell*, 135:1153–1156.
39. Feist AM, Herrgard MJ, Thiele I, Reed JL, Palsson BO (2009) Reconstruction of biochemical networks in microorganisms. *Nat Rev Microbiol*, 7:129–143.
40. Ong S-E, et al. (2009) Identifying the proteins to which small-molecule probes and drugs bind in cells. *Proc Natl Acad Sci USA*, 106:4617–4622.